

[Au(CN)₄][−] as Both an Intramolecular and Intermolecular Bidentate Ligand with [(tmeda)Cu(μ-OH)] Dimers: from Antiferro- to Ferromagnetic Coupling in Polymorphs

Michael J. Katz, Carolyn J. Shorrock, Raymond J. Batchelor, and Daniel B. Leznoff*

Department of Chemistry, Simon Fraser University, 8888 University Drive, Burnaby, British Columbia V5A 1S6, Canada

Received September 5, 2005

Two polymorphic products, [$\{\text{Cu}(\text{tmeda})(\mu\text{-OH})\}_2\text{Au}(\text{CN})_4][\text{Au}(\text{CN})_4]$ (**1**) and $[\text{Cu}(\text{tmeda})(\mu\text{-OH})\text{Au}(\text{CN})_4]_2$ (**2**), were synthesized from $\{\text{Cu}(\text{tmeda})(\mu\text{-OH})\}_2\text{X}_2$ (tmeda = *N,N,N',N'*-tetramethylethylenediamine, X = ClO_4^- , BF_4^-) and 2 equiv of $\text{K}[\text{Au}(\text{CN})_4]$, and their X-ray structures were determined. Both compounds have $\{\text{Cu}(\text{tmeda})(\mu\text{-OH})\}_2^{2+}$ dimers with $[\text{Au}(\text{CN})_4]^-$ units bound in the axial positions. However, in **1**, two trans N-donor cyanides of each $[\text{Au}(\text{CN})_4]^-$ unit bind to adjacent copper(II) dimers, forming a 1-D chain, whereas complex **2** is molecular, with two mono-coordinated $[\text{Au}(\text{CN})_4]^-$ units. The 1-D polymorph **1** is formed from aqueous solution, while the molecular polymorph **2** is obtained with X = BF_4^- in methanol. The polymorphs have slightly different Cu–O–Cu angles, a key magnetostructural parameter, such that the 1-D chain **1**, with an angle of $96.6(2)^\circ$, shows ferromagnetic interactions with $2J = +57.5 \text{ cm}^{-1}$ and $g = 2.097$, whereas the molecular complex **2**, with an angle of $98.92(17)^\circ$, shows antiferromagnetic interactions with $2J = -143.6 \text{ cm}^{-1}$ and $g = 2.047$. A similar Cu(II) complex, $[\{\text{Cu}(\text{tmeda})(\mu\text{-OH})\}_2\text{Au}(\text{CN})_4][\text{ClO}_4] \cdot \text{MeOH}$ (**3**), was synthesized in methanol when X = ClO_4^- , in which the $[\text{Au}(\text{CN})_4]^-$ unit bridges the two Cu(II) centers within the dimer in an intramolecular fashion via cis N-donor cyanides. The average Cu–O–Cu angle of $98.4(2)^\circ$ in **3** generates antiferromagnetic interactions with $2J = -64.8 \text{ cm}^{-1}$ and $g = 2.214$. Complexes **1–3** represent the first examples of $[\text{Cu}(\text{tmeda})(\mu\text{-OH})]_2^{2+}$ dimers with Cu–O–Cu angles under 100° , thereby extending the range of $2J$ coupling constants for this moiety from 149 to 566 cm^{-1} . The switch to ferromagnetic interactions in **1** as a result of the coordinating, bridging $[\text{Au}(\text{CN})_4]^-$ anion suggests that cationic, dinuclear moieties that are typically antiferromagnetically coupled may, with an appropriate coordinating counterion, become ferromagnetic units.

Introduction

One of the attractions of metal–organic coordination polymer research is the modular nature of the synthetic process: a vast range of building blocks exist, and ideally, the properties of the chosen blocks dictate the structural, spectroscopic, and materials characteristics of the resulting self-assembled product.^{1–5} The use of bimetallic or metal-cluster moieties as nodes in these metal–organic framework reac-

tions can permit a greater flexibility in geometric, redox, and magnetic properties compared with mononuclear building blocks. Using this guiding principle and focusing on dinuclear systems, a range of homometallic and heterobimetallic units have been incorporated into coordination polymers, including mixed-valent ruthenium(II/III),^{6,7} dirhodium(II),^{8–11} carboxylate-bridged^{12–15} or formamidinate-bridged metal dimers,^{10,16} $\text{Ni}_2(\mu\text{-oxalato})$ units,¹⁷ and a selection of

* To whom correspondence should be addressed. Tel: 1-604-291-4887. Fax: 1-604-291-3765. E-mail: dleznoff@sfu.ca.

(1) Janiak, C. *Dalton Trans.* **2003**, 2781.
 (2) James, S. L. *Chem. Soc. Rev.* **2003**, 32, 276.
 (3) Chesnut, D. J.; Hagrman, D.; Zapf, P. J.; Hammond, R. P.; LaDuca, R.; Haushalter, R. C.; Zubieta, J. *Coord. Chem. Rev.* **1999**, 192, 737.
 (4) Decurtins, S.; Pellaux, R.; Antorrena, G.; Palacio, F. *Coord. Chem. Rev.* **1999**, 190–192, 841.
 (5) Ouahab, L. *Chem. Mater.* **1997**, 9, 1909.

(6) Miyasaka, H.; Clerac, R.; Campos-Fernandez, C. S.; Dunbar, K. R. *Inorg. Chem.* **2001**, 40, 1663 and references therein.
 (7) Aquino, M. A. *Coord. Chem. Rev.* **1998**, 170, 141.
 (8) Miyasaka, H.; Campos-Fernandez, C. S.; Clerac, R.; Dunbar, K. R. *Angew. Chem., Int. Ed.* **2000**, 39, 3831.
 (9) Miyasaka, H.; Campos-Fernandez, C. S.; Galan-Mascaros, J. R.; Dunbar, K. R. *Inorg. Chem.* **2000**, 39, 5870.
 (10) Cotton, F. A.; Lin, C.; Murillo, C. A. *Chem. Commun.* **2001**, 11.
 (11) Bonar-Law, R. P.; McGrath, T. D.; Singh, N.; Bickley, J. F.; Steiner, A. *Chem. Commun.* **1999**, 2457.

copper(II) dimers.^{18–24} These last units, particularly [Cu(ligand)(μ -OH)]₂²⁺ dimers, have received a great deal of attention historically in terms of exploring the correlation between various structural parameters and the resulting magnetism (magnetostructural correlations).^{25–28} Despite this, relatively few of these classic copper(II) dimers have been utilized as building blocks for coordination polymers.^{23,24,29}

The fact that some [Cu(ligand)(μ -OH)]₂²⁺ dimers show antiferromagnetic interactions whereas others show ferromagnetic interactions was observed by Hodgson and Hatfield³⁰ to empirically depend on one key structural parameter: the magnetic interaction parameter ($2J$) was a linear function of the Cu–O–Cu angle (φ) such that $2J = -74.53\varphi + 7270 \text{ cm}^{-1}$. On the basis of this correlation, for a Cu–O–Cu angle of greater than 97.55° , the overall magnetic behavior of a [Cu(ligand)(μ -OH)]₂²⁺ system should be antiferromagnetic, and it should be ferromagnetic for angles smaller than 97.55° . The span of angles that has been observed (94.5° – 104.1°) has correlated well to a wide range of $2J$ values, from large positive values of up to +172 to negative values as low as -509 cm^{-1} .³⁰ Recently, the influence of other geometric parameters on the $2J$ coupling, in particular the angle of the O–H bond out of the Cu₂O₂ plane (the oop angle), have also been examined theoretically; large oop angles are predicted to favor ferromagnetic interactions.^{31–33}

The choice of ligand, most of which are bidentate nitrogen donors, affects the key Cu–O–Cu angle (via the restraints

Table 1. Summary of Structural and Magnetic Properties of Selected [Cu(ligand)(μ -OH)]₂²⁺ Complexes (Ordered by Magnitude of the Observed Coupling Constant, $2J$)

ligand ^a	anion	Cu–O–Cu (deg)	Cu–Cu (Å)	$2J$ (cm ⁻¹)	ref(s)
bipy	NO ₃	95.6	2.847	+172	34, 69, 88
bipy	CF ₃ SO ₃	96.9–98.5	2.892, 2.920	+158, +17	70
dmbpy	CF ₃ SO ₃	94.5	2.838	+148	43
bipy	C ₄ O ₄	96.4	2.870	+145	50
tmpd	ClO ₄	no data	no data	+130	30
bipy	ClO ₄	96.94	2.870	+93	30, 89
tmeda	Au(CN)₄	96.6	2.8984	+57.5	this work
bipy	SO ₄	97.0	2.893	+49	90–95
bipy	PF ₆	96.5	2.914	+12	80
β -dmaep	ClO ₄	98.4	2.938	-2.3	73, 79
tmeda	Au(CN)₄/ClO₄	97.9/98.8	2.9262	-64.8	this work
eaep	ClO ₄	98.8/99.5	2.917	-130	71, 72, 96
tmeda	Au(CN)₄	98.92	2.937	-143.6	this work
2miz	ClO ₄	100.4	2.987, 2.993	-175	97, 98
α -dmaep	ClO ₄	100.4	2.935	-200	77, 96
tmeda	ClO₄	102.3	2.966	-360	30, 42
tmeda	NO₃	101.9	2.955	-367	28, 35, 36
α -teeda	ClO ₄	103.0	2.978	-410	27, 34, 37
tmeda	Cl	103.2	2.98	-463	38
β -teeda	ClO ₄	104.1	2.996	-469	28, 35, 36
tmeda	Br	104.1	3.000	-509	39–41

^a Ligand abbreviations: bipy = 2,2'-bipyridine, dmaep = 2-(2-dimethylaminoethyl)pyridine, dmbpy = 4,4'-dimethyl-2,2'-bipyridine, eaep = 2-(2-ethylaminoethyl)pyridine, teeda = *N,N,N',N'*-tetraethylethylenediamine, tmeda = *N,N,N',N'*-tetramethylethylenediamine, tmpd = *N,N,N',N'*-tetramethyl-*o*-phenylenediamine, 2miz = 2-methylimidazole.

of the chelate bite angle), as is observed in Table 1, which shows metrical parameters and $2J$ couplings for selected [Cu(ligand)(μ -OH)]₂²⁺ units. For example, the reported [Cu(tmeda)(μ -OH)]₂²⁺ dimers (tmeda = *N,N,N',N'*-tetramethylethylenediamine) all display relatively large Cu–O–Cu angles ($> 101^\circ$), and thus, relatively strong antiferromagnetic interactions are observed,^{27,28,30,34–42} while [Cu(bipy)(μ -OH)]₂²⁺ complexes (bipy = 2,2'-bipyridine) all display ferromagnetic interactions.⁴³

Table 1 also illustrates that using the same ligand, the $2J$ value will still vary depending on the counteranion, X. Weakly or mildly coordinating anions such as ClO₄⁻, NO₃⁻, SO₄²⁻, and CF₃SO₃⁻ systems can have a large impact on the observed $2J$ coupling constants. For example, in the [Cu(bipy)(μ -OH)]₂X₂ system, the $2J$ coupling constants span a range of 160 cm^{-1} , while for the [Cu(tmeda)(μ -OH)]₂X₂ system, a range of 149 cm^{-1} is observed (see Table 1). These fluctuations in the $2J$ value can be attributed to structural changes in the copper(II) dimers which are induced by the

- (12) Bourne, S. A.; Lu, J.; Mondal, A.; Moulton, B.; Zaworotko, M. J. *Angew. Chem., Int. Ed.* **2001**, *40*, 2111.
- (13) Kim, J.; Chen, B.; Reineke, T. M.; Li, H.; Eddaoudi, M.; Moler, D. B.; O'Keeffe, M.; Yaghi, O. M. *J. Am. Chem. Soc.* **2001**, *123*, 8239.
- (14) Eddaoudi, M.; Moler, D. B.; Li, H.; Chen, B.; Reineke, T. M.; O'Keefe, M.; Yaghi, O. M. *Acc. Chem. Res.* **2001**, *34*, 319.
- (15) Chisholm, M. H. *Acc. Chem. Res.* **2000**, *33*, 53.
- (16) Cotton, F. A.; Lin, C.; Murillo, C. A. *Acc. Chem. Res.* **2001**, *34*, 759.
- (17) Vitoria, P.; Muga, I.; Gutierrez-Zorrilla, J. M.; Luque, A.; Roman, P.; Lezama, L.; Zuniga, J. J.; Beitia, J. I. *Inorg. Chem.* **2003**, *42*, 960.
- (18) Paraschiv, C.; Andruh, M.; Ferlay, S.; Hosseini, M. W.; Kyritsakas, N.; Planeix, J.-M.; Stanica, N. *Dalton Trans.* **2005**, 1195.
- (19) Marin, G.; Tudor, V.; Kravtsov, V. C.; Schmidtman, M.; Simonov, Y. A.; Müller, A.; Andruh, M. *Cryst. Growth Des.* **2005**, *5*, 279.
- (20) Tudor, V.; Marin, G.; Kravtsov, V.; Simonov, Y. A.; Lipkowskij, J.; Brezeanu, M.; Andruh, M. *Inorg. Chim. Acta* **2003**, *353*, 35.
- (21) Chen, F.-T.; Li, D.-F.; Gao, S.; Wang, X.-Y.; Li, Y.-Z.; Zheng, L.-M.; Tang, W.-X. *Dalton Trans.* **2003**, 3283.
- (22) Mukherjee, P. S.; Maji, T. K.; Mallah, T.; Zangrando, E.; Randaccio, L.; Chaudhuri, N. R. *Inorg. Chim. Acta* **2001**, *315*, 249.
- (23) de Munno, G.; Julve, M.; Lloret, F.; Faus, J.; Verdager, M.; Caneschi, A. *Inorg. Chem.* **1995**, *34*, 157.
- (24) Yu, J.-H.; Bie, H.-Y.; Xu, J.-Q.; Lu, J.; Zhang, X. *Inorg. Chem. Commun.* **2004**, *7*, 1205.
- (25) Kahn, O. *Molecular Magnetism*; VCH: Weinheim, 1993.
- (26) Hodgson, D. J. *Prog. Inorg. Chem.* **1974**, *19*, 173.
- (27) Estes, E. D.; Hatfield, W. E.; Hodgson, D. J. *Inorg. Chem.* **1974**, *13*, 1654.
- (28) Hatfield, W. E. In *Magneto-Structural Correlations in Exchange Coupled Systems*; Willett, R. D., Gatteschi, D., Kahn, O., Eds.; Reidel: Dordrecht, The Netherlands, 1984; p 555 and references therein.
- (29) Leznoff, D. B.; Draper, N. D.; Batchelor, R. J. *Polyhedron* **2003**, *22*, 1735.
- (30) Crawford, V. H.; Richardson, H. W.; Wasson, J. R.; Hodgson, D. J.; Hatfield, W. E. *Inorg. Chem.* **1976**, *15*, 2107.
- (31) Ruiz, E.; Alemany, P.; Alvarez, S.; Cano, J. *J. Am. Chem. Soc.* **1997**, *119*, 1297.
- (32) Ruiz, E.; Alemany, P.; Alvarez, S.; Cano, J. *Inorg. Chem.* **1997**, *36*, 3683.
- (33) Hu, H.; Liu, Y.; Zhang, D.; Liu, C. *J. Mol. Struct.* **2001**, *546*, 73.

- (34) McGregor, K. T.; Watkins, N. T.; Lewis, D. L.; Drake, R. F.; Hodgson, D. J.; Hatfield, W. E. *Inorg. Nucl. Chem. Lett.* **1973**, *9*, 423.
- (35) Nasakkala, M. *Ann. Acad. Sci. Fenn. Ser. A2* **1977**, *5*.
- (36) Nasakkala, M. *Ann. Acad. Sci. Fenn., Ser. A2* **1977**, *54*.
- (37) Hatfield, W. E.; Piper, T. S.; Klabunde, U. *Inorg. Chem.* **1963**, *2*, 629.
- (38) Meinders, H. C.; Van Bolhuis, F.; Challa, G. *J. Mol. Catal.* **1979**, *5*, 225.
- (39) Mitchell, T. P.; Bernard, W. H. *Acta Crystallogr.* **1970**, *B26*, 2096.
- (40) Wasson, J. R.; Mitchell, T. P.; Bernard, W. H. *J. Inorg. Nucl. Chem.* **1968**, *30*, 2865.
- (41) Cole, B. J.; Brumage, W. H. *J. Chem. Phys.* **1970**, *53*, 4718.
- (42) Arcus, C.; Fivizzani, K. P.; Pavkovic, S. F. *J. Inorg. Nucl. Chem.* **1977**, *39*, 285.
- (43) van Albada, G. A.; Mutikainen, I.; Turpeinen, U.; Reedijk, J. *Inorg. Chim. Acta* **2001**, *324*, 273 and references therein.

counterion via ligation to the copper(II) center, hydrogen-bonding to the O–H moiety, or even weak crystal-packing forces.

Most counterions employed to date with [Cu(ligand)(μ -OH)]₂²⁺ cations are simple units which were not chosen/ designed to link the copper(II) dimers together. Bridging anions such as cyanometalates, which are among the most popular and versatile building blocks in the coordination polymer field,^{44–48} have scarcely been employed with copper(II) dimer cations. The potential for increases in dimensionality could also produce further magnetic interaction pathways; this has been observed in 1-D chains of Cu(II) dimers through the use of bridging neutral ligands^{23,49} and less commonly through bridging anion coordination.⁵⁰ Continuing our interest in d¹⁰ and d⁸ cyanometalate-based coordination polymers^{29,51–59} and noting that the reaction of a (bipy)Cu(II) unit with weakly coordinating Hg(CN)₂ led to supramolecular systems containing [Cu(bipy)(μ -OH)]₂²⁺ dimers,²⁹ we turned to the examination of the reaction of the mildly coordinating d⁸-[Au(CN)₄][–] cyanometalate in conjunction with the related [Cu(tmeda)(μ -OH)]₂²⁺ dimer cation. The results reported here show the high sensitivity to reaction conditions, in the form of polymorphic products, and also illustrate the strong influence of coordinating counterions on the magnetic properties of the cation: the new range of 2J values for [Cu(tmeda)(μ -OH)]₂²⁺ spreads over 566 cm^{–1}, extending into the ferromagnetic regime.

Experimental Section

General Procedures and Physical Measurements. All manipulations were performed in air using purified solvents. The amine ligand tmeda and all other reagents were obtained from commercial

- (44) Dunbar, K. R.; Heintz, R. A. *Prog. Inorg. Chem.* **1997**, *45*, 283 and references therein.
- (45) Iwamoto, T. *Supramolecular Chemistry in Cyanometalate Systems*. In *Comprehensive Supramolecular Chemistry*; Lehn, J.-M., Atwood, J. L., Davies, J. E. D., MacNicol, D. D., Vogtle, F., Alberti, G. T. B., Eds.; Pergamon Press: Oxford, 1996; Vol. 7, pp 643–690 and references therein.
- (46) Ohba, M.; Okawa, H. *Coord. Chem. Rev.* **2000**, *198*, 313.
- (47) Cernak, J.; Orendac, M.; Potocnak, I.; Chomic, J.; Orendacova, A.; Skorsepa, J.; Feher, A. *Coord. Chem. Rev.* **2002**, *224*, 51.
- (48) Verdager, M.; Bleuzen, A.; Marvaud, V.; Vaissermann, J.; Seuleiman, M.; Desplanches, C.; Scuille, A.; Train, C.; Garde, R.; Gelly, G.; Lomenech, C.; Rosenman, I.; Veillet, P.; Cartier, C.; Villain, F. *Coord. Chem. Rev.* **1999**, *190–192*, 1023.
- (49) Chiari, B.; Hatfield, W. E.; Piovesana, O.; Tarantelli, T.; Ter Haar, L. W.; Zanazzi, P. F. *Inorg. Chem.* **1983**, *22*, 1468.
- (50) Castro, I.; Faus, J.; Julve, M.; Verdager, M.; Monge, A.; Gutierrez-Puebla, E. *Inorg. Chim. Acta* **1990**, *170*, 251.
- (51) Leznoff, D. B.; Xue, B.-Y.; Batchelor, R. J.; Einstein, F. W. B.; Patrick, B. O. *Inorg. Chem.* **2001**, *40*, 6026.
- (52) Leznoff, D. B.; Xue, B.-Y.; Stevens, C. L.; Storr, A.; Thompson, R. C.; Patrick, B. O. *Polyhedron* **2001**, *20*, 1247.
- (53) Leznoff, D. B.; Xue, B.-Y.; Stevens, C. L.; Storr, A.; Thompson, R. C.; Patrick, B. O. *Chem. Commun.* **2001**, 259.
- (54) Draper, N. D.; Batchelor, R. J.; Sih, B. C.; Ye, Z.-G.; Leznoff, D. B. *Chem. Mater.* **2003**, *15*, 1612.
- (55) Draper, N. D.; Batchelor, R. J.; Leznoff, D. B. *Cryst. Growth Des.* **2004**, *4*, 621.
- (56) Draper, N. D.; Batchelor, R. J.; Aguiar, P. M.; Kroeker, S.; Leznoff, D. B. *Inorg. Chem.* **2004**, *43*, 6557.
- (57) Lefebvre, J.; Batchelor, R. J.; Leznoff, D. B. *J. Am. Chem. Soc.* **2004**, *126*, 16117.
- (58) Shorrock, C. J.; Xue, B.-Y.; Kim, P. B.; Batchelor, R. J.; Patrick, B. O.; Leznoff, D. B. *Inorg. Chem.* **2002**, *41*, 6743.
- (59) Shorrock, C. J.; Jong, H.; Batchelor, R. J.; Leznoff, D. B. *Inorg. Chem.* **2003**, *42*, 3917.

sources and used as received. The μ -hydroxo copper(II) dimers [Cu(tmeda)(μ -OH)]₂(ClO₄)₂ and [Cu(tmeda)(μ -OH)]₂(BF₄)₂ were prepared according to published methods.^{30,60} IR spectra were obtained using a Thermo Nicolet Nexus 670 FT-IR spectrometer at a 1 cm^{–1} resolution. Microanalyses (C, H, N) were performed at Simon Fraser University by Mr. Miki Yang.

Variable-temperature magnetic susceptibility data were collected using a Quantum Design SQUID MPMS-XL7 Evercool magnetometer working down to 1.8 K at 1 T field strength. All data were corrected for the diamagnetism of the sample holder and the constituent atoms (by use of Pascal constants).²⁵

CAUTION: Although we have experienced no difficulties, perchlorate salts are potentially explosive and should only be used in small quantities and handled with care.

Preparation of the 1-D Chain polymorph [Cu(tmeda)(μ -OH)]₂Au(CN)₄[Au(CN)₄] (1). The dimer [Cu(tmeda)(μ -OH)]₂(ClO₄)₂ (48 mg, 0.081 mmol) was added to 20 mL of water. To the resulting blue solution was added a 5 mL aqueous solution of K[Au(CN)₄] (68 mg, 0.20 mmol) dropwise with stirring. This mixture was left to stir for 10 min, at which point a light blue precipitate began to form. After being stirred for one hour, the precipitate was separated by filtration, washed with 1 mL of water, and then air-dried overnight to yield a blue powder of **1**. Yield: 45 mg (56%). Anal. Calcd for C₂₀H₃₄N₁₂Au₂Cu₂O₂: C, 24.13; H, 3.44; N, 16.88. Found: C, 24.28; H, 3.42; N, 16.73. IR (KBr): 3601, 3453, 3017, 2990, 2937, 2904, 2854, 2817, 2193 (ν_{CN} , w), 2181 (ν_{CN} , w), 2173 (ν_{CN} , vw), 1469, 1285, 1245, 1124, 1044, 1021, 1001, 952, 807, 767, 594, 498, 415 cm^{–1}. X-ray quality crystals were obtained from the slow evaporation of the remaining solution. The IR spectra of the precipitate and the crystals are identical.

Preparation of the Molecular Polymorph [Cu(tmeda)(μ -OH)-Au(CN)₄] (2). The dimer [Cu(tmeda)(μ -OH)]₂(BF₄)₂ (57 mg, 0.10 mmol) was added to 15 mL of methanol and stirred vigorously for 1 h. To the resulting green solution was added a 5 mL methanolic solution of K[Au(CN)₄] (68 mg, 0.20 mmol), and the KBF₄ precipitate was filtered. If the remaining solution is stirred, a precipitate of **2** forms within 15 min, which was washed with <1 mL of methanol and air-dried overnight. Yield: 71 mg (71%). Anal. Calcd for C₂₀H₃₄N₁₂Au₂Cu₂O₂: C, 24.13; H, 3.44; N, 16.88. Found: C, 23.66; H, 3.27; N, 17.08. IR (KBr): 3597, 3011, 2987, 2874, 2943, 2921, 2856, 2816, 2208 (ν_{CN} , w), 2194 (ν_{CN} , w), 2182 (ν_{CN} , w), 1470, 1284, 1279, 1242, 1198, 1124, 1108, 1045, 1018, 1001, 952, 910, 873, 807, 769, 594, 498, 412 cm^{–1}. If the filtrate is not stirred after mixing/filtration and the solution is slowly concentrated by ~25% via evaporation, X-ray quality blue crystals of **2** are obtained after 3 days. The IR spectra of the precipitate and the crystals are identical.

Preparation of [Cu(tmeda)(μ -OH)]₂Au(CN)₄[ClO₄]·MeOH (3). The dimer [Cu(tmeda)(μ -OH)]₂(ClO₄)₂ (57 mg, 0.10 mmol) was added to 15 mL of methanol and stirred vigorously for 1 h. To the resulting green solution was added a 5 mL methanolic solution of K[Au(CN)₄] (68 mg, 0.2 mmol), resulting in an immediate light blue precipitate (primarily KClO₄), which was filtered and discarded. The remaining filtrate was left to slowly evaporate (covered with perforated Parafilm), yielding large X-ray quality blue crystals of **3** over 2 weeks. The crystals were separated from the solution (volume of solution decreased by approximately 1/2), were washed with <1 mL of methanol and air-dried overnight. Yield: 63 mg (76%). Anal. Calcd for C₁₆H₃₄N₈AuCu₂ClO₆·CH₃OH: C, 24.71; H, 4.64; N, 13.57. Found: C, 24.55; H, 4.56; N,

- (60) Handley, D. A.; Hitchcock, P. B.; Lee, T. H.; Leigh, G. J. *Inorg. Chim. Acta* **2001**, *316*, 59.

Table 2. Summary of Crystallographic Data^a

	1	2	3
formula	C ₂₀ H ₃₄ N ₁₂ Au ₂ Cu ₂ O ₂	C ₂₀ H ₃₄ N ₁₂ Au ₂ Cu ₂ O ₂	C ₁₇ H ₃₈ N ₈ AuClCu ₂ O ₇
fw	995.60	995.60	826.05
space group	P $\bar{1}$ (No. 2)	P $\bar{1}$ (No. 2)	P2 ₁ /m (No. 11)
a, Å	9.7135(17)	8.465(2)	8.4529(13)
b, Å	10.5792(19)	10.274(2)	15.7403(15)
c, Å	17.429(2)	10.468(2)	11.307(1)
α , deg	76.411(13)	64.35(2)	90
β , deg	82.953(13)	76.27(2)	95.03(1)
γ , deg	64.964(14)	79.26(2)	90
V, Å ³	1576.8(5)	793.6(3)	1498.6(3)
Z	2	1	2
ρ_{calc} , g/cm ³	2.097	2.083	1.831
μ , cm ⁻¹	106	105	64.2
T (K)	293	293	293
R, R _w (I > 2.5 σ (I)) ^b	0.023, 0.024	0.027, 0.033	0.027, 0.028

^a Enraf-Nonius CAD-4 diffractometer, Mo K α radiation ($\lambda = 0.71069$ Å), graphite monochromator. ^b Function minimized $\sum w(|F_o| - |F_c|)^2$ where $w^{-1} = \sigma^2(F_o) + nF_o^2$ ($n = 0.0001$ for **1**, 0.000081 for **2** and 0.000169 for **3**), $R = \sum ||F_o| - |F_c|| / \sum |F_o|$, $R_w = (\sum w(|F_o| - |F_c|)^2 / \sum w|F_o|^2)^{1/2}$.

13.80. IR (KBr): 3578, 3410, 3010, 2986, 2937, 2906, 2852, 2812, 2187 (ν_{CN} , w), 1469, 1461, 1291, 1283, 1246, 1091, 1045, 1021, 1003, 951, 807, 767, 638, 625, 492, 413 cm⁻¹. If the solution is stirred after the filtration step, a powder of **3** forms over several hours; the IR spectra of the powder and the single-crystals are identical.

X-ray Crystallographic Analysis. Crystallographic data for all structures are collected in Table 2. All crystals were mounted on glass fibers using epoxy adhesive. Using the diffractometer control program DIFRAC⁶¹ and an Enraf Nonius CAD4F diffractometer, data ranges were recorded as listed in the crystallographic information format (CIF) file. The data were corrected empirically for the effects of absorption, and data reduction for all compounds included corrections for Lorentz and polarization effects.

For all compounds, coordinates and anisotropic displacement parameters for the non-hydrogen atoms were refined. The hydrogen atoms on carbon and oxygen atoms in all complexes were placed in calculated positions (d C–H 0.95 Å; d O–H 1.00 Å), and their coordinate shifts were linked with those of the respective carbon or oxygen atoms during refinement. Isotropic thermal parameters for these hydrogen atoms were initially assigned proportionately to the equivalent isotropic thermal parameters of their respective carbon or oxygen atoms. Subsequently, the isotropic thermal parameters for the hydrogen atoms of CH₂, CH₃, or OH groups were, respectively, constrained to have identical shifts during refinement. However, for the –OH group in **2** and **3**, the hydrogen atom was found from the Fourier difference map and its position refined with isotropic thermal parameters to reasonable values and errors. The ClO₄⁻ oxygen atoms in **3** are disordered around the Cl site. An extinction parameter was included in the final cycles of full-matrix least-squares refinement of **1**. The final refinements, using observed data ($I_o \geq 2.5\sigma(I_o)$) included **1** = 350 parameters for 4006 data; **2** = 179 parameters for 3343 data; **3** = 198 parameters for 2408 data. Selected bond lengths and angles for all compounds are found in Tables 3–5.

The programs used for all absorption corrections and data reduction of **1–3** were from the NRCVAX Crystal Structure System.⁶² The structures were solved and refined using CRYSTALS.⁶³ Diagrams were made using ORTEP-3.⁶⁴ Complex scat-

tering factors for neutral atoms were used in the calculation of structure factors.⁶⁵

Results

Synthetic Methods. The reaction of K[Au(CN)₄] with the preformed [Cu(tmeda)(μ -OH)]₂X₂ dimer^{30,60} forms a series of related products depending on the anion, X, and the solvent used (X = ClO₄⁻ or BF₄⁻). In water, the addition of K[Au(CN)₄] to [Cu(tmeda)(μ -OH)]₂X₂ yields a complex (**1**) with the formula [Cu(tmeda)(μ -OH)]₂[Au(CN)₄]₂. In methanol, with X = BF₄⁻, another complex (**2**) with the same empirical formula but different IR spectrum is obtained, while if X is changed to ClO₄⁻, a third product (**3**) that retains 1 equiv of perchlorate anion is isolated from methanol. Single crystals were readily isolated for all three complexes, and their structures are described below. Note that if a copper(II) salt and the tmeda ligand are used as starting materials (i.e., instead of the preformed μ -OH dimer), only mixtures of these can be isolated.

The ν_{CN} bands of the infrared spectra of complexes **1–3** are much weaker than those generally observed for coordination polymers incorporating different cyanometalate building blocks and exhibit relatively smaller shifts upon N-donor cyanide binding; this feature has been previously observed in other [Au(CN)₄]⁻-based systems.^{17,59} However, the ν_{CN} peaks are sufficiently diagnostic that complexes **1–3** can be differentiated and identified; IR spectra of solved single crystals were initially obtained to ensure that the IR spectrum of only one compound or polymorph was sampled. Thus, **1** shows three ν_{CN} peaks at 2193, 2181, and 2173 cm⁻¹, slightly blue- or red-shifted vs K[Au(CN)₄] (2189 cm⁻¹). Complex **2** shows a triplet of equal intensity at 2208, 2194, and 2182 cm⁻¹, while **3** shows a single ν_{CN} peak at 2187 cm⁻¹, as well as a strong ClO₄⁻ peak.

Structure of the 1-D Chain [Cu(tmeda)(μ -OH)]₂Au(CN)₄[Au(CN)₄] (1**).** The X-ray crystal structure of **1** is depicted in Figures 1 and 2, with the corresponding bond

(61) Gabe, E. J.; White, P. S.; Enright, G. D. *DIFRAC A Fortran 77 Control Routine for 4-Circle Diffractometers*; N. R. C.: Ottawa, 1995.

(62) Gabe, E. J.; LePage, Y.; Charland, J.-P.; Lee, F. L.; White, P. S. *J. Appl. Crystallogr.* **1989**, *22*, 384.

(63) Betteridge, P. W.; Carruthers, J. R.; Cooper, R. I.; Prout, K.; Watkin, D. J. *J. Appl. Crystallogr.* **2003**, *36*, 1487.

(64) Farrugia, L. J. *J. Appl. Crystallogr.* **1997**, *30*, 565.

(65) *International Tables for X-ray Crystallography*. Kynoch Press: Birmingham, UK (present distributor Kluwer Academic Publishers: Boston, MA), Vol. IV, p 99.

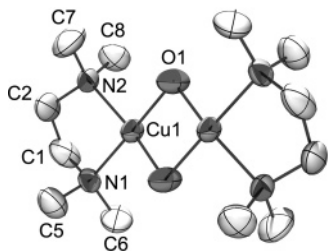


Figure 1. Structure of the [Cu(tmeda)(μ-OH)]₂²⁺ cation of [{Cu(tmeda)(μ-OH)}₂Au(CN)₄][Au(CN)₄][−] (**1**). Hydrogen atoms have been omitted for clarity (ORTEP, 50% ellipsoids).

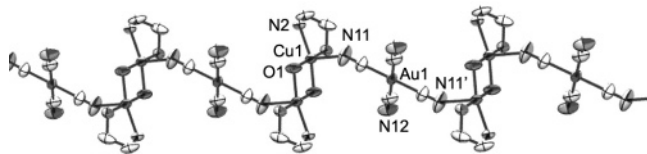


Figure 2. Extended structure of the 1-D chain of [{Cu(tmeda)(μ-OH)}₂Au(CN)₄]⁺ cations in **1**. Hydrogen atoms and methyl groups have been omitted for clarity (ORTEP, 50% ellipsoids).

Table 3. Selected Bond Lengths (Å) and Angles (deg) for [Cu(tmeda)(μ-OH)]₂Au(CN)₄[Au(CN)₄][−] (**1**)

Cu(1)–N(1)	2.023(5)	Cu(1)–N(2)	2.050(5)
Cu(1)–N(11)	2.392(7)	Cu(1)–O(1)	1.942(4)
Cu(1)–Cu(1) ^a	2.9041(15)	Cu(1)–O(1)′	1.949(4)
Au(1)–C(11)	1.988(7)	Au(1)–C(12)	1.984(9)
Au(3)–C(33)	1.988(8)	Au(3)–C(34)	1.976(7)
N(34)*–Au(1)	3.062(7)		
Cu(1)–O(1)–Cu(1)′	96.6(2)	N(1)–Cu(1)–N(2)	86.6(2)
N(1)–Cu(1)–N(11)	94.03(16)	N(2)–Cu(1)–N(11)	100.8(2)
N(1)–Cu(1)–O(1)	175.6(2)	N(2)–Cu(1)–O(1)	94.22(19)
N(11)–Cu(1)–O(1)	88.0(3)	O(1)–Cu(1)–O(1)′	83.4(2)
C(11)–N(11)–Cu(1)	148.8(8)	Au(1)–C(11)–N(11)	176.6(7)
C(31)–Au(3)–C(33)	179.4(3)	C(32)–Au(3)–C(34)	178.3(3)
C(34)*–N(34)*–Au(1)	163.5(7)		

^a Symmetry transformation: ′ ≡ 1 – x, 2 – y, 1 – z; * ≡ x + 1, y, z.

lengths and angles collected in Table 3. The X-ray crystal structure reveals the expected copper(II) hydroxo-bridged dimer cation, as depicted in Figure 1. There are two crystallographically unique half-dimer cations in the asymmetric unit, but the structural parameters are essentially identical for both. The square planar geometry about the copper atom is slightly distorted due to the chelating amine (N(1)–Cu(1)–N(2) = 86.6(2)°), but bond distances are all within the expected range (Cu–N range = 2.009(5)–2.051(5) Å and Cu–O range = 1.925(4)–1.950(4) Å) when compared with previously published [Cu(tmeda)(μ-OH)]₂²⁺ units, as well as other μ-hydroxo-bridged Cu(II) dimers (Table 1 refs). The distance between Cu(II) centers is 2.8984(15) Å, also within the range of 2.847–3.000 Å seen in other μ-hydroxo-bridged Cu(II) dimers and higher than the 2.61–2.65 Å range observed for complexes in which direct Cu–Cu bonding is postulated.^{66–68} Thus, the structural parameters of the dimer are quite similar to the previously observed [Cu(tmeda)(μ-OH)]₂²⁺ units, with the exception of the critical Cu–O–Cu angle: The Cu(1)–O(1)–Cu(1)′ angle in **1** is

96.6(2)°, whereas the lowest Cu–O–Cu angle reported to date for a [Cu(tmeda)(μ-OH)]₂²⁺ unit is 102.3(4)°.^{30,42} This acute angle in **1** indicates the possibility of ferromagnetic exchange between the paramagnetic Cu(II) centers, as suggested by the Hatfield and Hodgson equation.³⁰ This angle is particularly small as compared to the same dimer in the presence of counterions such as perchlorate, chloride, and bromide, all of which are observed to be strongly antiferromagnetic (Table 1). Note that the O(1)–H hydrogen atom could not be unambiguously located in **1** and thus the angle of the O–H bond vs the Cu₂O₂ plane (the oop angle) could not be determined.

The dimer cations are further coordinated by an N-donor cyanide from the [Au(CN)₄][−] anion, as seen in Figure 2. Anion coordination of this type has only been previously observed with oxygen donor anions in hydroxo-bridged Cu(II) dimer complexes.^{28,69–73} The Cu(1)–N(11) distance of 2.394(7) Å completes the square-pyramidal coordination sphere of the Cu(II) atom. This coordination results in the formation of a 1-D chain (Figure 2). An additional [Au(CN)₄][−] unit (Au(3), not shown) exhibits a N(34)⋯Au(1) interaction, thereby weakly linking it to the 1-D chain containing Au(1). This pendant [Au(CN)₄][−] unit does not interact with any Cu(II) dimer, either via direct ligation or by hydrogen-bonding with the O–H moiety.

Although 1-D chains of Cu(II) dimers have been observed in the literature,^{19,20,23,49,50,74} they usually occur through neutral bridging ligands such as bipyridyl-type units. A small number of other anion-bridged 1-D chains of hydroxo-bridged copper(II) dimers have been reported, including [Cu(bipy)(μ-OH)]₂(C₄O₄)·5.5H₂O, in which a planar squarate anion coordinates in a trans fashion through oxygen donors to two dimer molecules, thus propagating the chain,⁵⁰ and {[Cu(bipy)(μ-OH)(Cl)]₂Hg(CN)₂}·2H₂O, which forms a 1-D chain of [Cu(bipy)(μ-OH)]₂²⁺ dimers through a trans chloride bridging square-planar [μ-Cl₂Hg(CN)₂]^{2−} unit.²⁹ Hydrogen-bonding between copper(II) dimers and cyanometalate anions has been observed to self-assemble polymeric systems,⁷⁵ and divergent dicarboxylate ligands have also been utilized to connect copper(II) dimer nodes.⁷⁶

Structure of the Molecular Polymorph [Cu(tmeda)(μ-OH)Au(CN)₄]₂ (2). Crystals of **2**, which have a very similar morphology to **1**, were isolated by slow evaporation of a methanolic solution containing [Cu(tmeda)(μ-OH)]₂(BF₄)₂ and K[Au(CN)₄]. The X-ray crystal structure of **2** is depicted in Figure 3, with the corresponding bond lengths and angles

(69) Tadsanaprasittipol, A.; Kraatz, H.-B.; Enright, G. D. *Inorg. Chim. Acta* **1998**, *278*, 143.

(70) Castro, I.; Faus, J.; Julve, M.; Bois, C.; Real, J. A.; Lloret, F. *J. Chem. Soc., Dalton Trans.* **1992**, 47.

(71) Jeter, D. Y.; Lewis, D. L.; Hempel, J. C.; Hodgson, D. J.; Hatfield, W. E. *Inorg. Chem.* **1972**, *11*, 1958.

(72) Lewis, D. L.; Hatfield, W. E.; Hodgson, D. J. *Inorg. Chem.* **1972**, *11*, 2216.

(73) Lewis, D. L.; Hatfield, W. E.; Hodgson, D. J. *Inorg. Chem.* **1974**, *13*, 147.

(74) Manaka, H.; Yamada, I.; Yamaguchi, K. *J. Phys. Soc. Jpn.* **1997**, *66*, 564.

(75) Grasa, G.; Tuna, F.; Gheorghe, R.; Leznoff, D. B.; Rettig, S. J.; Andruh, M. *New J. Chem.* **2000**, *24*, 615.

(76) Pascu, M.; Andruh, M.; Müller, A.; Schmidtman, M. *Polyhedron* **2004**, *23*, 673.

(66) Mann, F. G.; Watson, H. R. *J. Chem. Soc.* **1958**, 2772.

(67) Barclay, G. A.; Kennard, C. H. L. *J. Chem. Soc.* **1961**, 5244.

(68) Hanic, F.; Stempelova, D.; Hanicova, K. *Acta Crystallogr.* **1964**, *17*, 633.

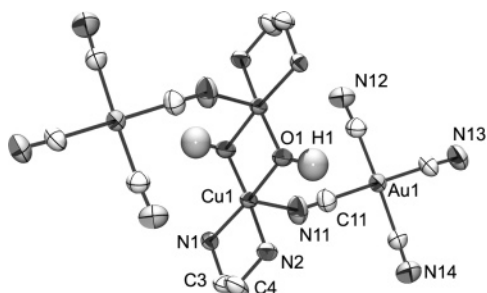


Figure 3. Structure of molecular $[\text{Cu}(\text{tmeda})(\mu\text{-OH})\text{Au}(\text{CN})_4]_2$ (**2**). Methyl groups and tmeda hydrogen atoms have been omitted for clarity (ORTEP, 50% ellipsoids).

Table 4. Selected Bond Lengths (Å) and Angles (deg) for $[\text{Cu}(\text{tmeda})(\mu\text{-OH})\text{Au}(\text{CN})_4]_2$ (**2**)

Cu(1)–N(1)	2.035(4)	Cu(1)–N(2)	2.059(4)
Cu(1)–O(1)	1.929(4)	Cu(1)–N(11)	2.435(6)
Cu(1)–Cu(1) ^a	2.9371(13)	Cu(1)–O(1)′	1.936(4)
Au(1)–C(11)	1.986(7)	Au(1)–C(12)	1.986(6)
Au(1)–C(13)	1.992(6)	Au(1)–C(14)	1.995(6)
Cu(1)–O(1)–Cu(1)′	98.92(17)	N(1)–Cu(1)–N(2)	86.71(17)
N(1)–Cu(1)–N(11)	93.4(2)	N(2)–Cu(1)–N(11)	96.3(2)
N(1)–Cu(1)–O(1)	174.72(19)	N(2)–Cu(1)–O(1)	95.15(16)
N(11)–Cu(1)–O(1)	91.3(2)	O(1)–Cu(1)–O(1)′	81.08(17)
C(11)–N(11)–Cu(1)	145.0(6)	C(11)–Au(1)–C(13)	178.5(3)

^a Symmetry transformation: ′ ≡ −x, 1 − y, 1 − z.

collected in Table 4. The X-ray crystal structure reveals the expected hydroxo-bridged dimer cation, similar to that seen in Figure 1 with only slight differences in bond lengths and angles, except for the key Cu(1)–O(1)–Cu(1)′ angle, which is 98.92(17)°. This is higher than that observed in **1**, and thus, **2** would be expected to show antiferromagnetic interactions, as opposed to the predicted ferromagnetic interactions of **1**. The hydroxide hydrogen position was found from the Fourier difference map and refined, and thus, the oop angle of 47.8° could be determined.

As in **1**, the $[\text{Au}(\text{CN})_4]^-$ anion is coordinated to the apical site of the square-pyramidal Cu(II) atom (Figure 3), though with a slightly longer bond distance (Cu(1)–N(11) = 2.435(6) Å). Unlike in **1**, however, this anion does not further coordinate to another cationic dimer unit, and thus, the structure is molecular rather than a 1-D chain.

There are significantly more Cu(II) dimer units that show apical coordination of anions without propagation into a 1-D chain. Most, however, contain apical Cu–O bonds, such as is observed in many $[\text{Cu}(\text{bipy})(\mu\text{-OH})_2]^{2+}$ dimers (Table 1) with nitrate, sulfate, and triflate anions (whereby Cu–O_{apical} = 2.363–2.453 Å). Other Cu(II) dimers also show similar coordination with the above anions (Cu–O_{apical} = 2.56–2.72 Å).^{72,77} No such coordination has been observed for tmeda-based copper(II) dimers, nor with nitrogen donor anions. Many of the aforementioned anions are considered to be “semi-coordinated” due to their relatively long bond lengths as compared to apical Cu–O bonds in other complexes.⁷⁸ The Cu(1)–N(11) bond distance of 2.435(6) Å is shorter than the above Cu–O bond lengths and within the range of

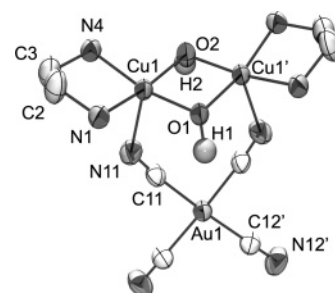


Figure 4. Structure of the cationic moiety $[\{\text{Cu}(\text{tmeda})(\mu\text{-OH})\}_2\text{Au}(\text{CN})_4]^+$ in $[\{\text{Cu}(\text{tmeda})(\mu\text{-OH})\}_2\text{Au}(\text{CN})_4][\text{ClO}_4]\cdot\text{MeOH}$ (**3**). Methyl groups, tmeda hydrogen atoms and a noncoordinated MeOH molecule have been omitted for clarity (ORTEP, 50% ellipsoids).

Table 5. Selected Bond Lengths (Å) and Angles (deg) for $[\{\text{Cu}(\text{tmeda})(\mu\text{-OH})\}_2\text{Au}(\text{CN})_4][\text{ClO}_4]\cdot\text{MeOH}$ (**3**)

Cu(1)–N(1)	2.030(4)	Cu(1)–N(4)	2.049(4)
Cu(1)–N(11)	2.462(4)	Cu(1)–Cu(1) ^a	2.9262(11)
Cu(1)–O(1)	1.940(3)	Cu(1)–O(2)	1.927(3)
Au(1)–C(11)	1.993(6)	Au(1)–C(12)	2.003(5)
O(1)–H(1)	0.861(5)	O(2)–H(2)	1.012(4)
O(1)–O(21)*	2.913(33)	O(2)–O(11)	2.918(12)
O(21)*–H(1)	2.166(37)	O(11)–H(2)	1.928(11)
N(1)–Cu(1)–N(4)	86.08(16)	N(1)–Cu(1)–O(1)	93.63(15)
N(1)–Cu(1)–O(2)	166.82(18)	N(4)–Cu(1)–O(1)	167.03(19)
N(4)–Cu(1)–O(2)	95.93(15)	O(1)–Cu(1)–O(2)	81.50(14)
Cu(1)–O(1)–Cu(1)′	97.9(2)	Cu(1)–O(2)–Cu(1)′	98.83(19)
C(11)′–Au(1)–C(12)	177.0(2)	O(1)–H(1)–O(21)*	145(1)
O(2)–H(2)–O(11)	165.2(5)		

^a Symmetry transformations: ′ ≡ x, 1/2 − y, z; * ≡ x − 1, y, z.

other Cu–N apical bonds of square-pyramidal Cu(II) complexes.

Structure of $[\{\text{Cu}(\text{tmeda})(\mu\text{-OH})\}_2\text{Au}(\text{CN})_4][\text{ClO}_4]\cdot\text{MeOH}$ (3**).** Crystals of **3** were formed by slow evaporation of a methanolic solution containing 1 equiv of $[\text{Cu}(\text{tmeda})(\mu\text{-OH})_2](\text{ClO}_4)_2$ and 2 equiv of $[\text{Au}(\text{CN})_4]^-$. The ClO_4^- peak (characteristically strong and broad, at approximately 1100 cm^{-1}) uniquely identified **3** as compared with **1**, for which this band was completely absent. The X-ray crystal structure of the cation of **3** is depicted in Figure 4, with the corresponding bond lengths and angles collected in Table 5. The X-ray crystal structure reveals the expected hydroxo-bridged dimer cation (Figure 1), with similar Cu–N(amine) and Cu–O bond lengths and angles to the dimers observed in **1** and **2**.

The Cu(1)–O(1)–Cu(1)′ and Cu(1)–O(2)–Cu(1) angles are 97.9(2)° and 98.8(2)°, respectively. The OH hydrogen atoms were located and refined, and a relatively large O–H oop angle of 57.6° was determined; this sizable O–H tilt is likely due to the weak hydrogen-bonding interaction of the O–H proton with the ClO_4^- anion (see Table 5).³¹

The $[\text{Au}(\text{CN})_4]^-$ anion is coordinated through N-donor cyanides to the Cu(II) centers, with an apical Cu(1)–N(11) distance of 2.462(4) Å, thus yielding a square-pyramidal coordination geometry at the Cu(II) center. However, in this complex, the $[\text{Au}(\text{CN})_4]^-$ anion is bound through two cis N-donor cyanide atoms of the $[\text{Au}(\text{CN})_4]^-$ moiety to the two Cu(II) atoms of a single dimer cation, as seen in Figure 4. This is a relatively rare form of anion bridging for hydroxo-bridged Cu(II) dimers but has been observed with the triflate anion in $[\text{Cu}(\text{dmbpy})(\mu\text{-OH})\text{CF}_3\text{SO}_3]_2$ and the perchlorate

(77) Lewis, D. L.; McGregor, K. T.; Hatfield, W. E.; Hodgson, D. J. *Inorg. Chem.* **1974**, *13*, 1013.

(78) Brown, D. S.; Lee, J. D.; Melsom, B. G. A.; Hathaway, B. J.; Procter, I. M.; Tomlinson, A. A. G. *Chem. Commun.* **1967**, 369.

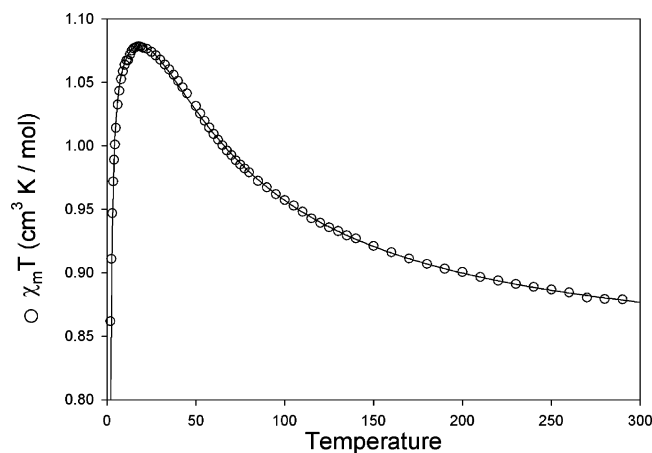


Figure 5. Temperature dependence of $\chi_M T$ for **1**. The solid line corresponds to the theoretical fit (see text).

anion in α -[Cu(dmaep)(μ -OH)ClO₄]₂; in these cases, two anions intramolecularly bridge on either side of the dimer to yield octahedral copper(II) centers.^{43,79} In **3**, the copper(II) centers are five-coordinate, with only a single [Au(CN)₄]⁻ anion bound to each: the ClO₄⁻ anion and methanol solvent both remain uncoordinated. In the tetranuclear cluster [Cu(bipy)(μ -OH)₄(PF₆)₄], each pair of copper(II) ions is weakly coordinated by a PF₆⁻ anion in a fashion similar to the [Au(CN)₄]⁻ in **3**.⁸⁰

Magnetic Properties. For **1–3** the temperature (*T*) dependence of the molar magnetic susceptibilities (χ_M) was measured from 1.8 to 300 K. For the 1-D chain of [{Cu(tmeda)(μ -OH)}₂Au(CN)₄][Au(CN)₄] (**1**), the observed $\chi_M T$ value is 0.88 cm³ K mol⁻¹ at 300 K (Figure 5), slightly higher than that expected for two magnetically isolated Cu(II) centers. Upon decreasing the temperature, $\chi_M T$ increases to a maximum of 1.08 cm³ K mol⁻¹ at 18 K and then decreases to 0.86 cm³ K mol⁻¹ at 2 K (Figure 5). The increase is characteristic of ferromagnetic intradimer interactions, and the maximum $\chi_M T$ value corresponds to a fully ferromagnetically coupled pair of *S* = 1/2 centers (i.e., an *S* = 1 system). The decrease below 18 K is likely a result of either interdimer antiferromagnetic interactions or zero-field splitting of the ferromagnetically coupled *S* = 1 dimer.

Accordingly, the data was fit using the Bleaney–Bowers model^{25,81} for *S* = 1/2 dimers, with $\mathbf{H} = -2J\mathbf{S}_1 \cdot \mathbf{S}_2$ and an additional molecular field parameter *zJ'* to account for the presumably much weaker interdimer interactions.^{29,50} This fit, depicted as a solid line in Figure 5, results in the best-fit values of $2J = +57.5 \pm 0.4$ cm⁻¹, *g* = 2.0969 ± 0.0005 and *zJ'* = -0.34 ± 0.02 cm⁻¹. Thus, the ferromagnetically coupled Cu(II) dimers may weakly interact antiferromagnetically via the diamagnetic cyanoaurate(III) bridge; other diamagnetic metal centers are known to be capable of mediating magnetic interactions.^{53,58,82,83} The particularly weak interdimer interaction in **1** could be attributed to the

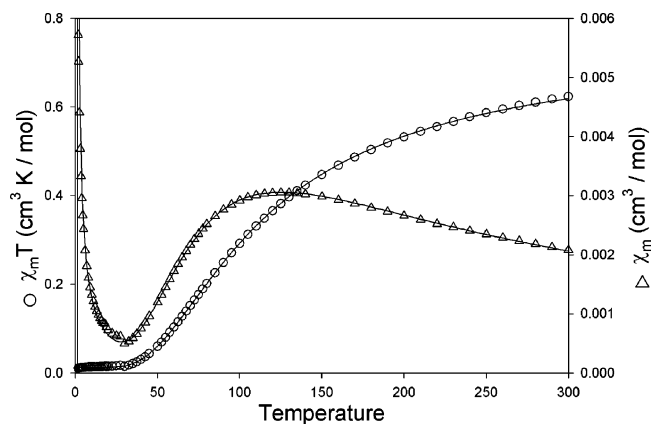


Figure 6. Temperature dependence of χ_M and $\chi_M T$ for **2**. The solid lines correspond to the theoretical fit (see text).

Jahn–Teller elongated connection that structurally holds the chain together but greatly reduces the efficiency of the magnetic overlap.⁵⁴ An equally reasonable fit can be obtained using the equation for a ferromagnetically coupled *S* = 1/2 dimer with zero-field-splitting (*D*) of the *S* = 1 ground state,²⁵ which yields comparable values of $2J = +57.2 \pm 0.4$ cm⁻¹, *g*_{av} = 2.069 ± 0.08, and *D* = 2.2 ± 0.3 cm⁻¹. However, this *D* value is unusually large for an *S* = 1 copper(II) dimer,²⁵ implying that intermolecular antiferromagnetic interactions are likely operative in **1** to some extent at low temperature.^{70,79,84}

The temperature dependence of the product $\chi_M T$ for the molecular polymorph **2** shows completely different characteristics compared to the 1-D polymorph, **1**; the $\chi_M T$ and χ_M vs *T* plots are shown in Figure 6. At 300 K, $\chi_M T = 0.62$ cm³ K mol⁻¹, significantly reduced compared to the $\chi_M T$ value of 0.75 cm³ K mol⁻¹ for two independent *S* = 1/2 centers. The $\chi_M T$ values continually drop with decreasing temperature, becoming nearly zero at 1.8 K, indicative of strong *antiferromagnetic* interactions within the hydroxo-copper(II) dimer; a broad maximum in the χ_M vs *T* plot between 100 and 125 K is also characteristic (a Curie tail is present in χ_M below 30 K due to a paramagnetic impurity). The data for **2** can be fit to a simple Bleaney–Bowers equation with a paramagnetic impurity (*P*) to yield best-fit values of $2J = -143.6 \pm 0.3$ cm⁻¹, *g* = 2.047 ± 0.016, and *P* = 3.61% ± 0.05; this fit is illustrated by the solid lines in Figure 6.

For [{Cu(tmeda)(μ -OH)}₂Au(CN)₄][ClO₄]·MeOH (**3**), $\chi_M T = 0.81$ cm³ K mol⁻¹ at 300 K, as expected for two independent Cu(II) centers. The $\chi_M T$ value decreases to a minimum of 0.016 cm³ K mol⁻¹ at 1.8 K, as depicted in Figure 7. As observed for **2**, this decrease is consistent with the presence of intradimer antiferromagnetic interactions, as is the characteristic maximum in the χ_M vs *T* graph at approximately 57 K (a Curie tail is also present at low *T*). The data can be fit (solid lines in Figure 7) using the

(79) McGregor, K. T.; Hodgson, D. J.; Hatfield, W. E. *Inorg. Chem.* **1976**, *15*, 421.

(80) Sletten, J.; Sorensen, A.; Julve, M.; Journaux, Y. *Inorg. Chem.* **1990**, *29*, 5054.

(81) Bleaney, B.; Bowers, K. D. *Proc. R. Soc. London, Ser. A* **1952**, *214*, 451.

(82) Oshio, H.; Watanabe, T.; Ohto, A.; Ito, T.; Nagashima, U. *Angew. Chem., Int. Ed. Engl.* **1994**, *33*, 670.

(83) Oshio, H.; Watanabe, T.; Ohto, A.; Ito, T.; Ikoma, T.; Tero-Kubota, S. *Inorg. Chem.* **1997**, *36*, 3014.

(84) Rodríguez, M.; Llobet, A.; Corbella, M.; Martell, A. E.; Reibenspies, J. *Inorg. Chem.* **1999**, *38*, 2328.

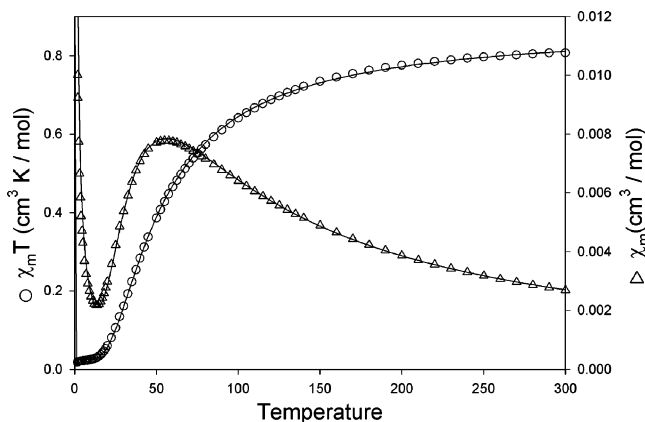


Figure 7. Temperature dependence of χ_M and $\chi_M T$ for **3**. The solid lines correspond to the theoretical fit (see text).

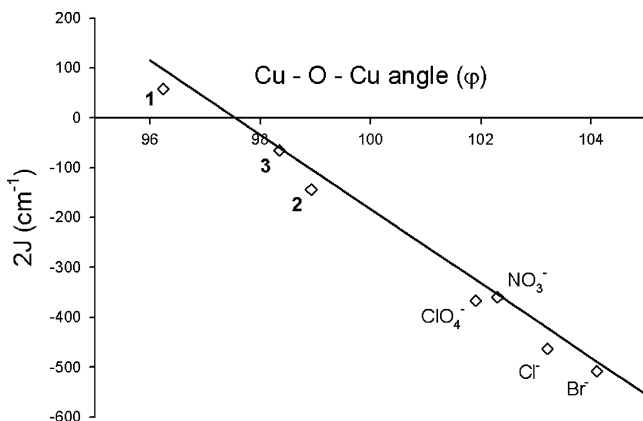


Figure 8. Plot of $2J$ vs Cu–O–Cu angle for $[\text{Cu}(\text{tmeda})(\mu\text{-OH})]_2\text{X}_2$ dimers with various anions (X). The solid line corresponds to the calculated Hodgson and Hatfield magnetostructural correlation.³⁰

Bleaney–Bowers model for $S = 1/2$ dimers with $\mathbf{H} = -2J\mathbf{S}_1 \cdot \mathbf{S}_2$ (assuming no interdimer interactions),²⁵ and including a paramagnetic impurity (P) resulting in the best-fit values of $2J = -64.82 \pm 0.02 \text{ cm}^{-1}$, $g = 2.214 \pm 0.001$, and $P = 6.74\% \pm 0.12$.

Discussion

Magnetostructural Correlations of $[\text{Cu}(\text{tmeda})(\mu\text{-OH})]_2^{2+}$ Dimers. Complexes **1–3** represent three new $[\text{Cu}(\text{tmeda})(\mu\text{-OH})]_2^{2+}$ dimers with a unique anionic unit. The magnetostructural correlation equation as proposed by Hodgson and Hatfield³⁰ can be applied to each complex, resulting in predicted $2J$ values of $+70.4$, -102.5 , and -63.75 cm^{-1} (based on the average Cu–O–Cu angles for **2** and **3**), respectively. The observed $2J$ values of $+57.5$, -143.6 , and -64.8 cm^{-1} for **1–3**, respectively, deviate moderately from the calculated values, as can be observed in the graphical representation in Figure 8. Upon including the data for **1–3**, the range of observed $2J$ coupling constants for $[\text{Cu}(\text{tmeda})(\mu\text{-OH})]_2^{2+}$ dimers is increased from 149 cm^{-1} to a remarkable 566 cm^{-1} , by far the largest range for a given ligand (Table 1).

Recently, it has been suggested that deviations from the Cu–O–Cu angle-based prediction can be attributed to the unaccounted-for effect of the oop hydrogen atom angle's influence on magnetic orbital overlap.^{31,32,85} Using this oop

angle, it has been predicted that if the O–H hydrogen atom remains in the Cu_2O_2 plane (i.e., $\text{oop} = 0^\circ$), most hydroxo-bridged Cu(II) dimers will show antiferromagnetic coupling, while if the oop angle is large (i.e., the hydrogen atom is significantly out of the plane), ferromagnetic interactions will result. In fact, the hydroxo-bridged Cu(II) dimers that have small Cu–O–Cu angles tend to show (theoretically and experimentally) large oop angles of the hydrogen atom, suggesting that these two parameters may be correlated.^{31,32,85} Such observations and recent investigations suggest that this oop angle contributes to minor fluctuations or perturbations from the previously proposed Cu–O–Cu angle magnetism predictions primarily for systems where the Cu–O–Cu is between 95° and 99° .³¹ However, the difficulties associated with locating the exact position of hydrogen atoms from X-ray data have precluded this discussion with respect to the majority of $[\text{Cu}(\text{ligand})(\mu\text{-OH})]_2\text{X}_2$ systems. For **2** and **3**, the oop angles of 47.8° and 57.5° , respectively, were successfully determined and they do not appear to have substantially altered the general correlation between the observed $2J$ coupling constant and the predicted $2J$ value on the basis of the Cu–O–Cu angle alone. Indeed, an examination of the collated data in Figure 8 indicates that, for the $[\text{Cu}(\text{tmeda})(\mu\text{-OH})]_2\text{X}_2$ system, deviations from the Hodgson–Hatfield magnetostructural correlation are generally toward *more antiferromagnetic* values. Calculations have shown that the combination of a Cu–O–Cu angle of below 98° and an oop angle of well over 50° are required to yield ferromagnetic interactions; apparently, the combination of Cu–O–Cu angle = 98.35° (average) and oop angle = 57.5° found for **3** is insufficient to alter the negative sign of the observed $2J$ coupling.³¹

Significantly, complexes **1–3** represent the first $[\text{Cu}(\text{tmeda})(\mu\text{-OH})]_2^{2+}$ complexes with Cu–O–Cu angles below 100° . Furthermore, complex **1** is the first ferromagnetic $[\text{Cu}(\text{tmeda})(\mu\text{-OH})]_2^{2+}$ complex. This is also the first instance where a series of $[\text{Cu}(\text{ligand})(\mu\text{-OH})]_2^{2+}$ dimers with a specific capping ligand has exhibited both antiferromagnetic and ferromagnetic interactions. The effect of anion choice has been shown to influence the magnetic properties only in cases where the anion is bound to the dimer.³² This suggests that appropriate use of coordinating anions, including other cyanometalates, could be instrumental in accessing a wider range of copper(II) dimers with different magnetic interactions. Thus, those copper(II) dimers which typically show antiferromagnetic interactions with non-coordinating anions (Table 1) are potentially convertible into ferromagnetically coupled units upon reaction with coordinating anionic ligands. Calculations have predicted that for μ -hydroxo Cu(II) dimer systems with an ethylenediamine ligand (or multiple NH_3 ligands) changes in anion choice could produce a wide range of $2J$ couplings (both ferromagnetic and antiferromagnetic within a series of dimer complexes), although no such dimers have ever been successfully synthesized.³² Other factors affecting magnetic properties,

(85) Ruiz, E.; Alvarez, S.; Alemany, P. *Chem. Commun.* **1998**, 2767.

such as the basicity of the ligand, Cu–O distances, and hinge distortion of asymmetric dimers have all been explored.³²

Polymorphic Products. The multiple coordination modes of the $[\text{Au}(\text{CN})_4]^-$ unit have been recently shown to be useful for increasing structural dimensionality.^{17,59} In the case of 1-D **1** and molecular **2**, differences in the coordination mode define two polymorphs, i.e., they have the same empirical formula but crystallize in a different fashion depending on the solvent and Cu(II) salt counteranion used. Note that neither solvent nor counteranion actually is incorporated into the final product; hence, **1** and **2** are “true” polymorphs, as opposed to “pseudo-polymorphs” that differ in structure due to included solvent.^{86,87} The choice of $\text{X} = \text{BF}_4^-$ vs ClO_4^- counterion in the $[\text{Cu}(\text{tmeda})(\mu\text{-OH})_2\text{X}_2]$ starting material plays no role in directing the aqueous reactions but controls the product isolated from methanol. It is likely that the solubility of **3** in methanol is quite low once formed, facilitating its isolation; in contrast, the putative BF_4^- analogue of **3** likely remains soluble, allowing the reaction to progress to full replacement of BF_4^- for $[\text{Au}(\text{CN})_4]^-$, i.e., polymorph **2**. In addition to the solvent of crystallization and counterion choice, factors such as the temperature, seed crystals, and reagent concentration all influence the formation of a particular polymorph.^{57,86,87}

- (86) Dunitz, J. D.; Bernstein, J. *Acc. Chem. Res.* **1995**, *28*, 193.
 (87) Bernstein, J. *Polymorphism in Molecular Crystals*; Oxford University Press: Oxford, 2002.
 (88) Majeste, R. J.; Meyers, E. A. *J. Phys. Chem.* **1970**, *74*, 3497.
 (89) Toofan, M.; Boushehri, A.; Ul-Haque, M. *J. Chem. Soc., Dalton Trans.* **1976**, 217.
 (90) Barnes, J. A.; Hatfield, W. E.; Hodgson, D. *J. Chem. Commun.* **1970**, 1593.
 (91) Casey, A. T.; Hoskins, B. F.; Whillans, F. D. *Chem. Commun.* **1970**, 904.
 (92) Casey, A. T. *Aust. J. Chem.* **1972**, *25*, 2311.
 (93) Hoskins, B. F.; Whillans, F. D. *J. Chem. Soc., Dalton Trans.* **1975**, 1267.
 (94) Barnes, J. A.; Hodgson, D. J.; Hatfield, W. E. *Inorg. Chem.* **1972**, *11*, 144.
 (95) McGregor, K. T.; Hodgson, D. J.; Hatfield, W. E. *Inorg. Chem.* **1973**, *12*, 731.
 (96) Krahmer, P.; Masser, M.; Staiger, K.; Uhlig, E. *Z. Anorg. Allg. Chem.* **1967**, *354*, 242.
 (97) Ivarsson, G. J. M. *Acta Chem. Scand.* **1979**, *A33*, 323.
 (98) Reedijk, J.; Kentsch, D.; Nieuwenhuijse, G. *Inorg. Chim. Acta* **1971**, *5*, 568.

The formation of multiple Cu(II) dimer-containing products from a single reaction system has been previously observed. The same aqueous solution of Cu^{2+} , NO_3^- , bpm (2,2'-bipyrimidine), and sodium carbonate was shown to produce crystals of both $[\text{Cu}_2(\text{bpm})(\text{H}_2\text{O})_2(\mu\text{-OH})_2](\text{NO}_3)_2$ and $[\text{Cu}_2(\text{bpm})(\text{H}_2\text{O})_2(\mu\text{-OH})_2(\text{NO}_3)_2] \cdot 2\text{H}_2\text{O}$ with undefined yields, whereas very slight changes to the reactant concentrations yielded primarily $[\text{Cu}_2(\text{bpm})_2(\text{H}_2\text{O})_2(\mu\text{-OH})_2(\text{NO}_3)_2] \cdot 4\text{H}_2\text{O}$ with undefined minimal yields (crystals were reportedly hand-picked) of $[\text{Cu}_2(\text{bpm})(\mu\text{-OH})_2(\text{NO}_3)_2] \cdot 2\text{H}_2\text{O}$.²³ This type of delicate equilibrium appears to be a common occurrence in the formation of hydroxo-bridged Cu(II) dimer systems.

Conclusions

Complexes **1–3** represent the first examples of $[\text{Cu}(\text{tmeda})(\mu\text{-OH})_2]^{2+}$ dimers where the Cu–O–Cu angles are lower than 100° ; **1** is thus the first such dimer that exhibits ferromagnetic coupling. This result suggests that coordinating anions, and particularly bridging anions, can greatly influence the magnetic properties of hydroxo-bridged Cu(II) dimers, enough to alter the sign of the $2J$ coupling constant; such manipulation may prove fruitful in other dinuclear systems as well. Indeed, the results presented here increase the $2J$ coupling range for $[\text{Cu}(\text{tmeda})(\mu\text{-OH})_2]^{2+}$ dimers to 566 cm^{-1} , attributable to counterion manipulation. Although the facile formation of polymorphs in the $[\text{Cu}(\text{tmeda})(\mu\text{-OH})_2]^{2+}$ - $[\text{Au}(\text{CN})_4]^-$ system is a complicating factor, if controllable as in the case of **1** and **2**, it also offers the opportunity to access a wider range of magnetic properties from the same building block.

Acknowledgment. Financial support from NSERC of Canada and the World Gold Council GROW program are gratefully acknowledged.

Supporting Information Available: Complete crystallographic data in CIF format for all three reported crystal structures. This material is available free of charge via the Internet at <http://pubs.acs.org>.

IC0515094